

## Delivery of Telomerase Reverse Transcriptase Small Interfering RNA in Complex with Positively Charged Single-Walled Carbon Nanotubes Suppresses Tumor Growth

Zhuohan Zhang,<sup>1</sup> Xiaoying Yang,<sup>3</sup> Yuan Zhang,<sup>1</sup> Bin Zeng,<sup>1</sup> Shujing Wang,<sup>3</sup> Tianhui Zhu,<sup>1</sup> Richard B.S. Roden,<sup>4</sup> Yongsheng Chen,<sup>3</sup> and Rongcun Yang<sup>1,2,4</sup>

**Abstract Purpose:** To determine whether -CONH-(CH<sub>2</sub>)<sub>6</sub>-NH<sub>3</sub><sup>+</sup>Cl<sup>-</sup> functionalized single-walled carbon nanotubes (SWNT) carrying complexed small interfering RNA (siRNA) can enter into tumor cells, wherein they release the siRNA to silence the targeted gene.

**Experimental Design:** -CONH-(CH<sub>2</sub>)<sub>6</sub>-NH<sub>3</sub><sup>+</sup>Cl<sup>-</sup> was used to mediate the conjugation of telomerase reverse transcriptase (TERT) siRNA to SWNTs. The ability of TERT siRNA delivered via SWNT complexes to silence the expression of TERT was assessed by their effects on the proliferation and growth of tumor cells both *in vitro* and in mouse models.

**Results:** The functionalized SWNTs -CONH-(CH<sub>2</sub>)<sub>6</sub>-NH<sub>3</sub><sup>+</sup>Cl<sup>-</sup> could facilitate the coupling of siRNAs that specifically target murine TERT expression to form the mTERT siRNA:SWNT+ complex. These functionalized SWNTs rapidly entered three cultured murine tumor cell lines, suppressed mTERT expression, and produced growth arrest. Injection of mTERT siRNA:SWNT+ complexes into s.c. Lewis lung tumors reduced tumor growth. Furthermore, human TERT siRNA:SWNT+ complexes also suppressed the growth of human HeLa cells both *in vitro* and when injected into tumors in nude mice.

**Conclusions:** -CONH-(CH<sub>2</sub>)<sub>6</sub>-NH<sub>3</sub><sup>+</sup>Cl<sup>-</sup> functionalized SWNTs carry complexed siRNA into tumor cells, wherein they release the siRNA from the nanotube sidewalls to silence the targeted gene. The -CONH-(CH<sub>2</sub>)<sub>6</sub>-NH<sub>3</sub><sup>+</sup>Cl<sup>-</sup> functionalized SWNTs may represent a new class of molecular transporters applicable for siRNA therapeutics.

The ability of functionalized single-walled carbon nanotubes (SWNT) to penetrate mammalian cells without apparent cytotoxicity suggests their applicability as carriers for internalization of drugs or delivery of vaccines. Oxidized SWNTs can be functionalized at their carboxylic groups with proteins, peptide, DNA, oligonucleotide, sugar moieties, polyoxide derivatives, etc.

(1–5). SWNTs functionalized with nucleic acids, such as small interfering RNA (siRNA) or DNA, show promise for application in gene therapy and gene interference (6). Telomerase is the key enzyme for the stabilization of chromosomes by adding TTAGGG repeats to the telomere ends (7, 8). Activation of telomerase is critical for immortalization and is detected in majority of malignant tumors but not in most normal somatic cells. Therefore, small-molecule inhibitors of telomerase activity or knockdown of telomerase expression represents attractive approaches for targeted cancer therapy. RNA interference (RNAi) is a powerful tool to dissect functional consequences of target inactivation in mammalian cells and model organisms (8). Delivery of siRNA to target cells is complicated by the instability of siRNA, low uptake efficiency, and properties of their bioavailability. Thus, more efficient siRNA delivery methods are required to realize the potential of siRNA to address both basic biological questions and provide therapeutic benefit. In this study, we used -CONH-(CH<sub>2</sub>)<sub>6</sub>-NH<sub>3</sub><sup>+</sup>Cl<sup>-</sup> to mediate the conjugation of siRNA to SWNTs and examined the ability of telomerase reverse transcriptase (TERT) siRNA delivered via SWNT complexes to silence the expression of TERT and inhibit the proliferation and growth of tumor cells both *in vitro* and in mouse models.

**Authors' Affiliations:** <sup>1</sup>Department of Immunology, College of Medicine, <sup>2</sup>Key Laboratory of Bioactive Materials, Ministry of Education, and <sup>3</sup>Institute of Polymer Chemistry and Key Laboratory for Functional Polymer Materials, College of Chemistry, Nankai University, Tianjin, People's Republic of China and <sup>4</sup>Department of Pathology, Johns Hopkins University School of Medicine, Baltimore, Maryland Received 12/27/05; revised 4/2/06; accepted 5/4/06.

**Grant support:** Ministry of Science and Technology of China "863" Project grant 2003AA302640, Ministry of Education of China Postdoctoral Funding grant 20040055020, Tianjin City and Nankai University Funding National Science Foundation Funding grant 043803711. R.B.S. Roden was supported by Public Health Service grant P50 CA098252, American Cancer Society Research Scholar grant RSG MBC-103744, and Department of Defense grant OC010017.

The costs of publication of this article were defrayed in part by the payment of page charges. This article must therefore be hereby marked *advertisement* in accordance with 18 U.S.C. Section 1734 solely to indicate this fact.

**Note:** Supplementary data for this article are available at Clinical Cancer Research Online (<http://clincancerres.aacrjournals.org/>).

R. Yang and Y. Chen contributed equally to this work.

**Requests for reprints:** Yongsheng Chen, Institute of Polymer Chemistry and Key Laboratory for Functional Polymer Materials, College of Chemistry, Nankai University, Tianjin 300071, People's Republic of China. Phone: 86-22-23500693; Fax: 86-22-23499992; E-mail: yschen99@nankai.edu.cn.

© 2006 American Association for Cancer Research.

doi:10.1158/1078-0432.CCR-05-2831

### Materials and Methods

**Preparation of SWNTs: DNA labeled with FAM fluorescein (SWNTs-dsDNA-FAM).** To investigate the penetration of SWNTs in to tumor

cells, SWNTs were functionalized using DNA labeled with FAM fluorescein by the procedure of Hazani et al. (9). Functionalized SWNTs with ssDNA were characterized using transmission electron microscopy equipped with energy-dispersive X-ray spectroscopy (Tecnaï 20, FEI, Hillsboro, OR) and atomic force microscopy (Nanoscope multimode scanning probe microscope, Veeco, Woodbury, NY). SWNTs bound with captured ssDNA (SWNTs-sDNA; 50 mg/L) and the target DNA labeled with FAM (27  $\mu\text{mol/L}$ ) were added into boiling water and then cooled to 4°C to permit annealing. After washing, the resulting functionalized SWNTs-dsDNA-FAM was used in the following experiments. The fluorescence spectrum of SWNTs-sDNA hybridized with either complementary or noncomplementary FAM-labeled DNA was assayed using a FluoroMax-P (Jobin Yvon, Edison, NJ).

**siRNA design, synthesis, and transfection.** The siRNA sequences used for gene silencing of mouse TERT (mTERT) were designed using the protocol described on <http://www.ambion.com>. Specific mTERT sequences targeted are AACAGATCAAGAGCAGTAGTC (sequence 1) and AATATGTCAGACTCCTCAGGT (sequence 2). Specific human TERT (hTERT) sequences targeted are AAGCACTTCCTACTCCTCA (sequence 1) and AACACCAAGAAGTTCATCTCC (sequence 2). The nonsilencing control siRNA is an irrelevant siRNA with random nucleotides ACUATCUAA-GUUACTACCCCTT. Sequences were synthesized and annealed.

**Preparation of mTERT siRNA:SWNTs complexes mediated by  $-(\text{CONH}-(\text{CH}_2)_6-\text{NH}_3^+\text{Cl}^-)$  (mTERT siRNA:SWNTs+).** SWNTs were prepared using our previously described method (10) and then purified and shortened as in Hazani et al. (9). To prepare the positively charged SWNTs (SWNTs+), we first generated the *tert*-butyl *N*-(6-aminoethyl) carbamate (Boc-C<sub>6</sub>H<sub>12</sub>NH<sub>2</sub>) using a procedure reported by Far et al. (11). SWNT-COCl was prepared as described previously (12) from shortened SWNTs. SWNT-COCl (0.0691 g) and Boc-C<sub>6</sub>H<sub>12</sub>NH<sub>2</sub> (4.3 g) were then reacted in dimethylformamide at 90°C for 96 hours under argon. The SWNTs functionalized with Boc-protected amines in the previous step (SWNT-CONH-C<sub>6</sub>H<sub>12</sub>NH-Boc) were collected by filtration (0.1  $\mu\text{m}$ ) and washed twice with dioxane. Boc groups were removed using a procedure similar to that reported by Han et al. (13). A solution of HCl/dioxane (0.4 mL/9.6 mL) in a 25-mL round-bottomed flask equipped with a magnetic stir bar was cooled in an ice-water bath under argon, and then SWNT-CONH-C<sub>6</sub>H<sub>12</sub>NH-Boc (30 mg) was added with stirring. The ice bath was removed, and the mixture was stirred for 1 hour. The reaction mixture was collected by centrifugation and then washed twice with dioxane. Finally, aqueous HCl solution (6 mol/L) was added into the aqueous suspension of functionalized SWNTs, and the positively charged functionalized SWNTs were collected by standard centrifugation and membrane filtration (0.1  $\mu\text{m}$ ). This functionalization procedure for SWNTs avoids reaction of amino groups of 1,6-diaminohexane between different SWNTs and consequent aggregation. Indeed, SWNTs functionalized using this method better disperse in water than those produced by conventional methodology. The solubilized SWNTs were mostly individual tubes (nonaggregated) and small bundles as revealed by spectrometry and atomic force microscopy, respectively. The SWNT concentration in the solution after this process was estimated at 25 mg/L.

To prepare the siRNA functionalized SWNTs, the SWNT-CONH-(CH<sub>2</sub>)<sub>6</sub>-NH<sub>3</sub><sup>+</sup> (50-100 mg/L) was incubated with siRNA at 100 nmol/L for 1 hour in room temperature and then washed twice before use. The coupling of siRNA with SWNTs+ was assessed by transmission electron microscopy equipped with energy-dispersive X-ray spectroscopy, atomic force microscopy, and spectrophotometry (BioPhotometer, Eppendorf, Hamburg, Germany).

**Transfection of mTERT siRNA:SWNTs+ and SWNTs-dsDNA-FAM into tumor cells.** The siRNA:SWNTs+ complexes were added at 2 nmol/L (siRNA concentration) to cultures of human HeLa cells, mouse ovarian surface epithelial cell line 1H8, mouse cervical cancer cell line TC-1, Lewis lung carcinoma (LLC) tumor cells obtained from the American Type Culture Collection (Manassas, VA), Dr. Katherine Roby (Department of Anatomy and Cell Biology, University of Kansas Medical Center, Kansas City, KS; ref. 14), Dr. T.C. Wu (The Johns Hopkins

University School of Medicine, Baltimore, MD), and the Beijing Animal Center (Beijing, China), respectively] in 24-well plates. Specific mTERT siRNA:SWNTs+ or control mock siRNA:SWNTs+ or siRNA alone was added into each well, and cell growth was monitored daily. The level of TERT mRNA and the expression of TERT protein were analyzed by reverse transcription-PCR and Western blotting after 48 hours. FAM-DNA-SWNT was used to transfect tumor cells using similar methods.

**Reverse transcription-PCR analysis.** Total cellular RNA was prepared using Trizol reagent (Invitrogen, Carlsbad, CA) followed by RNA cleanup with RNeasy Mini kit (Qiagen, Valencia, CA) as recommended by the manufacturer. Reverse transcription-PCR was done by SuperScript one-step reverse transcription-PCR with Platinum Taq according to the protocol provided (Invitrogen). The primers used include the following: mTERT, 5'-ATGACCCGCGCTCCTCGTTGC and 3'-GACAG-CAGAGATGTGGAGCTG; hTERT, 5'-ATGCCGCGCGCTCCCGCTG and 3'-GCTCGCAGCGGGCAGTGCGT; and glyceraldehyde-3-phosphate dehydrogenase, 5'-ATGGTGAAAGTCGGTGTGAACGGATTGGC and 3'-CATCGAAGGTGGAAGAGTGGGAGTTGCTGT.

**Western blot analysis.** 1H8, TC-1, and LLC cells or HeLa tumor cells were harvested by centrifugation for 10 minutes at 600  $\times$  g. For Western blotting of TERT protein, nuclear extract was prepared according to a reported procedure (15) and then 100  $\mu\text{g}$  of nuclear extract were separated by 7.5% SDS-PAGE and transferred to nitrocellulose membrane. After blocking with 5% nonfat dry milk, the membrane was incubated with rabbit anti-TERT polyclonal antibody (1:200; Santa Cruz Biotechnology, Santa Cruz, CA). The protein-antibody complexes were detected using the peroxidase-conjugated secondary antibody (Boehringer Mannheim, Mannheim, Germany) and enhanced chemiluminescence (Amersham, Buckinghamshire, United Kingdom). As a loading control, actin was also assessed using anti-actin antibody (2G2, STI, Darmstadt, Germany).

**Telomerase activity assay.** A commercial telomerase PCR ELISA kit (Boehringer Mannheim) based on the telomeric repeat application protocol introduced by Kim et al. (16) was used to determine telomerase activity.

## Results and Discussion

**Penetration of SWNTs-dsDNA-FAM into different mouse tumor cells.** Several groups have described the ability of SWNTs to penetrate mammalian cells and to deliver cargos, such as small peptides, protein, and nucleic acid (2, 3). Here, we examined the ability of SWNTs functionalized with FAM fluorescently labeled short dsDNA (20 bp; SWNTs-dsDNA-FAM) to enter into three murine tumor cell lines. SWNTs functionalized with amino-modified DNA (SWNTs-sDNA) were prepared, and their structure was validated by transmission electron microscopy (Supplementary Fig. S1A1) and atomic force microscopy (data not shown). The presence of the fluorescently labeled short dsDNA after SWNTs-sDNA hybridized with FAM complement DNA was confirmed by fluorescence spectroscopy (Supplementary Fig. S1A2). When the SWNTs-dsDNA-FAM was incubated with 1H8, TC-1, and LLC tumor cells, its uptake could be clearly visualized by fluorescence microscopy at 4 hours (Supplementary Fig. S1B3, C3, and D3) and flow cytometry (Supplementary Fig. S1B4, C4, and D4). No obvious toxicity was observed grossly, consistent with previous reports (2, 17).

**Preparation of mTERT siRNA:SWNTs complexes mediated by  $-(\text{CONH}-(\text{CH}_2)_6-\text{NH}_3^+\text{Cl}^-)$ .** Because functionalized SWNTs penetrate mammalian cells without apparent cytotoxicity, we examined their potential application as a carrier for delivery of siRNA. Kam et al. (6) first reported conjugation of siRNA to SWNTs functionalized by noncovalent adsorption of phospholipids with polyethylene glycol (molecular weight of

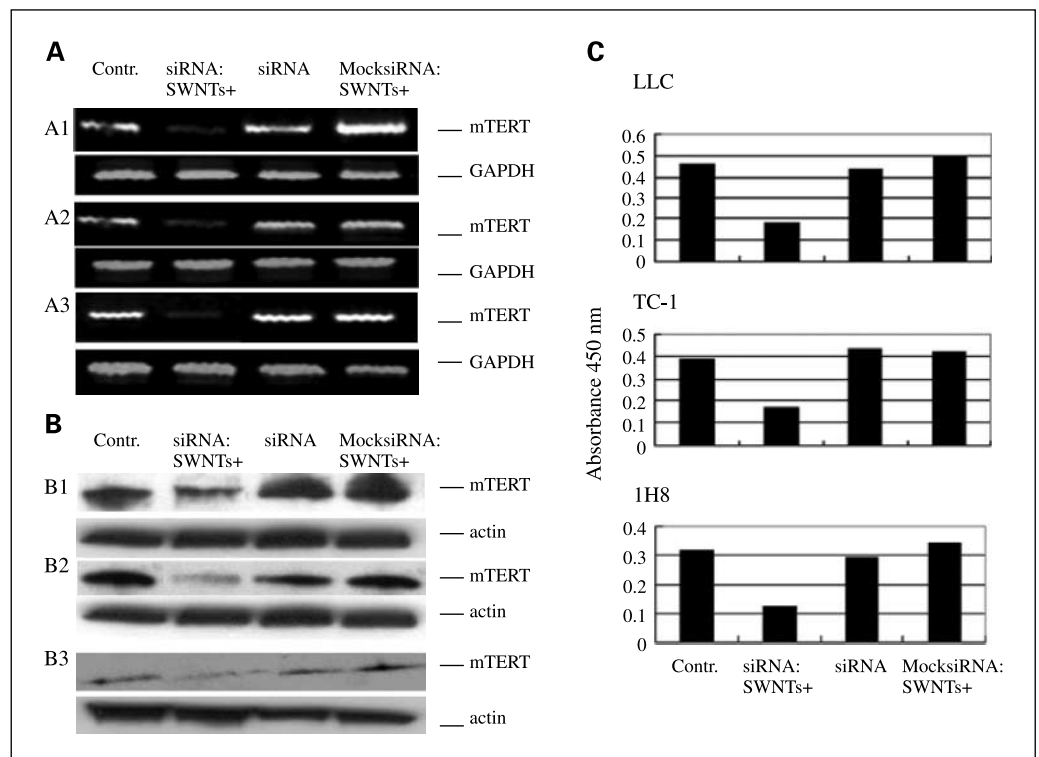
polyethylene glycol, 2,000) chains and terminal amine or maleimide groups. Here, we found that functionalization of SWNTs with the positively charged  $-\text{CONH}-(\text{CH}_2)_6-\text{NH}_3^+\text{Cl}^-$  group could effectively assist coupling of mTERT siRNA to oxidized SWNTs. Atomic force microscopy suggested the coupling of siRNA and SWNTs+ (Supplementary Fig. S2A). The binding of mTERT siRNA to oxidized SWNTs was shown by transmission electron microscopy equipped with energy-dispersive X-ray spectroscopy (Supplementary Fig. S2B). The energy-dispersive X-ray spectroscopy spectrum of the siRNA:SWNTs+ complex revealed a strong elemental phosphorus-associated peak (Supplementary Fig. S2B3), which is absent in the energy-dispersive X-ray spectroscopy spectrum of siRNA:SWNTs (Supplementary Fig. S2B2) and shortened SWNTs (Supplementary Fig. S2B1). Spectrophotometric analysis at 260 nm also showed that SWNTs conjugated with  $-\text{CONH}-(\text{CH}_2)_6-\text{NH}_3^+\text{Cl}^-$  promoted the coupling of siRNA to SWNTs (Supplementary Fig. S2C). Thus, positive charge functionalization not only promotes the coupling of protein and DNA with SWNTs (18) but also mediates the conjugation of siRNA with SWNTs.

**SWNTs mediated in vitro delivery of TERT siRNA into tumor cells to silence the TERT gene.** Although SWNTs transport biological molecules in the cells with no apparent ill effects on cell viability, it is unclear whether the mTERT siRNA:SWNTs+ complexes mediated by  $-\text{CONH}-(\text{CH}_2)_6-\text{NH}_3^+\text{Cl}^-$  could effectively exert RNAi. RNAi needs appropriate conformation to specifically bind its target sequence and a protein-RNA effector nuclease complex. This complex uses the siRNA as a template to recognize and cleave RNA targets with complementary sequence. Thus, we next investigated whether exogenous addition of mTERT siRNA:SWNTs complexes mediated by  $-\text{CONH}-(\text{CH}_2)_6-\text{NH}_3^+\text{Cl}^-$  could specifically exert RNAi on mTERT gene expression. Murine models of cervical carcinoma

(TC-1), ovarian carcinoma (1H8), and the lung carcinoma (LLC) all express a high level of mTERT mRNA and mTERT proteins. Addition of mTERT siRNA:SWNTs+ complexes reduced the cellular levels of both mTERT mRNA (Fig. 1A) and mTERT protein (Fig. 1B) in all three cell lines. As indicated in Fig. 1, treatment with siRNA alone, SWNTs, or SWNTs complexed with control siRNA by  $-\text{CONH}-(\text{CH}_2)_6-\text{NH}_3^+\text{Cl}^-$  did not significantly alter the level of either mTERT mRNA or mTERT protein. Reduced telomerase activity in mTERT siRNA:SWNTs+ transfected tumor cells further confirmed the successful delivery of active mTERT siRNA via functionalized SWNTs by  $-\text{CONH}-(\text{CH}_2)_6-\text{NH}_3^+\text{Cl}^-$  to silence mTERT (Fig. 1C).

**mTERT siRNA:SWNT+ complexes mediated by  $-\text{CONH}-(\text{CH}_2)_6-\text{NH}_3^+\text{Cl}^-$  suppressed the proliferation of mouse tumor cells in vitro.** Telomerase is a cellular RNA-dependent DNA polymerase that maintains the tandem telomeric TTAGGG repeats at eukaryotic chromosome ends (7), and TERT is its proteinaceous catalytic subunit (19). Thus, TERT plays a critical role in tumor development and growth through the maintenance of telomere structure. The first example of telomerase-targeted gene therapy was reported by Feng et al. (20). Antisense RNA targeting the first 185 nucleotides of the TERT molecule was induced into HeLa cells and caused progressive telomere shortening and, eventually, cell crisis (20). Therefore, we sought to determine the effect of TERT siRNA:SWNT+ complexes on the levels of TERT and growth of LLC, TC-1, and 1H8 tumor cells. The three cell lines were plated ( $0.5 \times 10^5$  per well of 24-well plate) and, after an overnight incubation, treated with 2 nmol/L TERT siRNA:SWNTs+ complexes. The mTERT siRNA:SWNTs+ clearly suppressed the growth of LLC, TC-1, and 1H8 and reduced the cell number after 6 days of incubation, whereas addition of TERT siRNA alone or mock siRNA:SWNTs+ complexes did not significantly affect cell growth (Fig. 2). The

**Fig. 1.** Specific gene silencing induced by mTERT siRNA:SWNT+ complexes in tumor cells. **A**, level of mTERT transcripts after treatment of LLC (A1), TC-1 (A2), and 1H8 (A3) tumor cells for 24 hours with 2 nmol/L of mTERT siRNA:SWNTs+, mTERT siRNA alone, and mock siRNA:SWNTs+ versus untreated control cells. GAPDH, glyceraldehyde-3-phosphate dehydrogenase. **B**, protein level of mTERT and actin in LLC (B1), TC-1 (B2), and 1H8 (B3) tumor cells treated as in (A). Data are representative of three independent experiments. **C**, as for (B), but telomerase activity was assayed.



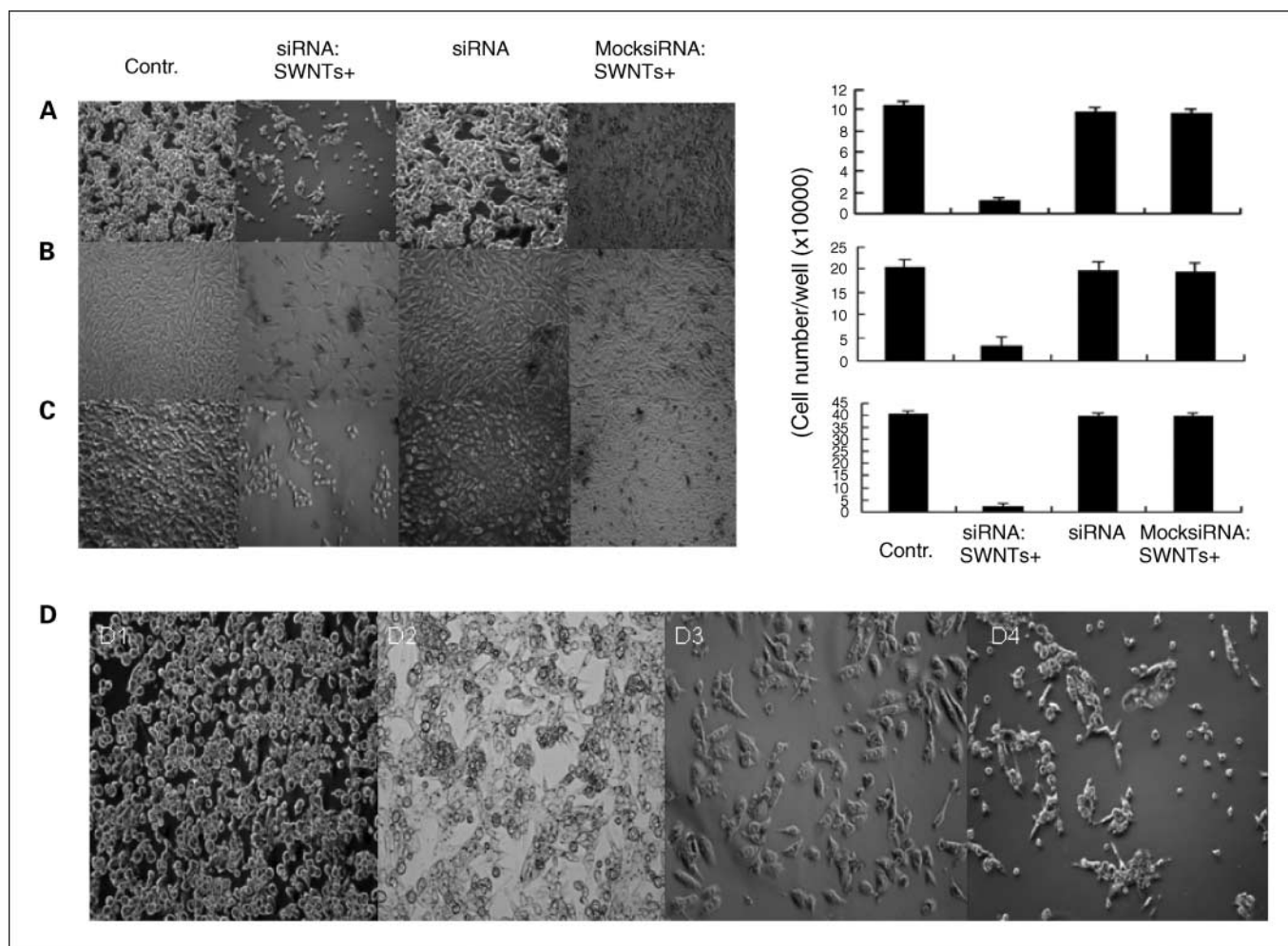


**Fig. 2.** *In vitro* suppression of tumor cell proliferation and induction of senescence by mTERT siRNA:SWNT+ complexes. Micrographs of LLC (A), TC-1 (B), and 1H8 (C) tumor cells ( $2 \times 10^5$  cultured per well in a 24-well plate) either untreated or treated with mTERT siRNA:SWNTs+, siRNA alone, or mock siRNA:SWNTs+. The cell number was counted after culture for 6 days. D, appearance of LLC cells before treatment (D1), after 2 days (D2), after 4 days (D3), and after 6 days of treatment with mTERT siRNA:SWNTs (D4).

growth kinetics of mTERT siRNA:SWNTs+ transfected cells initially did not differ from those of untreated, siRNA alone, or mock siRNA:SWNTs+ transfected control cells regardless of the cell lines used. However, by 48 hours, the cells treated with mTERT siRNA:SWNT+ complexes mediated by  $-\text{CONH}-(\text{CH}_2)_6-\text{NH}_3^+\text{Cl}^-$  showed an almost complete inhibition of proliferation. Under phase-contrast microscopy, LLC, TC-1, and 1H8 cells treated with mTERT siRNA:SWNTs+ complexes showed distinctive morphologic features associated with senescence, including growth arrest, enlargement, and a vacuolated cytoplasm (Fig. 2). These findings were absent from the TERT siRNA alone or mock siRNA:SWNTs+ transfected control cells. Similar findings were described previously in the murine RenCa renal carcinoma line on ectopic expression of mutant mTERT (21).

Safety and biocompatibility are major concerns when introducing a gene therapy to patients. Several groups have reported that relatively pure, well-solubilized short carbon nanotubes seem nontoxic once internalized into mammalian cells. Indeed, as shown in Fig. 2, mTERT siRNA:SWNTs+ did not adversely affect cell biology or exhibit obvious toxicity in three cell lines.

**Suppression of tumor growth by intralesional injection of mTERT siRNA:SWNT+ complexes mediated by  $-\text{CONH}-(\text{CH}_2)_6-\text{NH}_3^+\text{Cl}^-$ .** Because incubation of tumor cell lines with mTERT siRNA:SWNT+ complexes knocked down mTERT expression, inhibited cell proliferation, and promoted cell senescence *in vitro*, we explored their activity on *in vivo* tumor growth. mTERT siRNA:SWNTs+ complexes versus mTERT siRNA alone or mock siRNA:SWNTs+ complexes were injected into LLC tumor tissue once the tumor had attained dimensions of  $5 \times 5 \times 5 \text{ mm}^3$ . Injection of mTERT siRNA:SWNT+ complexes at either a single site or multiple sites inhibited the growth of tumor and induced the senescence of tumor cells (Fig. 3); the average tumor weight harvested at day 7 was significantly reduced compared with untreated ( $P < 0.0002$ , ANOVA) and injection of control mTERT siRNA alone or mock siRNA:SWNT+ complexes (Fig. 3). The effectiveness of mTERT siRNA:SWNT+ complexes at multiple sites was more effective in retarding tumor growth than injection at a single point (Fig. 3A and B). Most tumor cells from tumor tissue injected with SWNTs-dsDNA-FAM were fluorescent, indicating penetration of SWNTs (Fig. 3D). Furthermore, injection of mTERT

siRNA:SWNT+ into tumor tissue also induced senescence as determined by measurement of the marker of senescence-associated  $\beta$ -galactosidase in this but not the other treatment groups (Fig. 3E).

Because there may be differences in the biology of telomeres and nanotube uptake in human versus murine tumor cells, we explored the potential of hTERT siRNA:SWNT+ complexes to inhibit the growth of the human cervical cancer cell line HeLa. Specific gene silencing induced by hTERT siRNA:SWNT+ complexes was observed in human HeLa cells at the transcript (Fig. 4A), protein (Fig. 4B), and functional level (Fig. 4C) and triggered senescence as indicated by the expression of senescence-associated  $\beta$ -galactosidase in >80% of treated but not control cells (Fig. 4D and E). Importantly, intralesional

injection of hTERT siRNA:SWNT+ complexes significantly and specifically suppressed human HeLa cell growth versus control (Fig. 4F-H). The transduction of both the human melanoma line LOX and the human transitional bladder carcinoma line UM-UC-3 with mutant hTERT via lentivirus also produced a rapid inhibition of cell growth, although the responses of the colon cancer line HCT116, breast cancer line MCF-7, and prostate cancer line LNCAP were slower (22). Similarly, antisense-mediated hTERT inhibition specifically reduces the growth of the four human bladder cancer lines EJ28, 5637, J82, and HT1197 (23). Importantly, coexpression of hTERT siRNA sensitizes tumor cells to the effects of mutant hTERT (22). Given the rapid response of the cell lines to TERT knockdown, it is possible that telomeric shortening is not the only

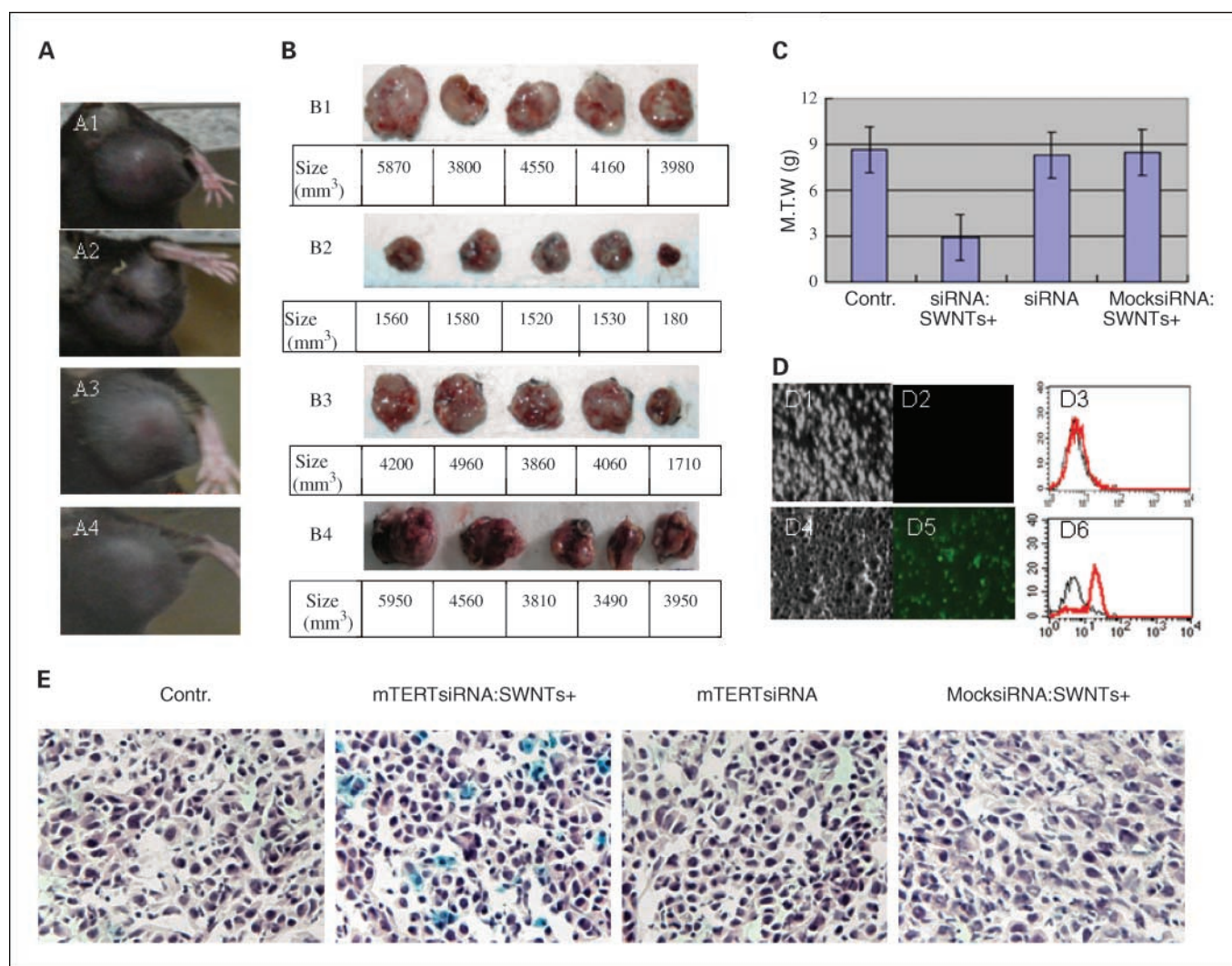


**Fig. 3.** Injection of mTERT siRNA:SWNT+ complexes suppresses LLC tumor growth *in vivo*. **A**, LLC tumor size at day 7 after injection at a single site. **A1**, control; **A2**, mTERT siRNA:SWNT+ complexes; **A3**, mTERT siRNA alone; **A4**, mock siRNA:SWNT+ complexes. LLC tumor cells ( $1 \times 10^6$  per mouse) were injected s.c into the right leg (five mice per group). After 1 week, when the dimensions of tumor reached approximately  $5 \times 5 \times 5$  mm<sup>3</sup>, mTERT siRNA:SWNTs, siRNA alone, or mock siRNA:SWNT+ complexes were injected into tumors at a single site (100  $\mu$ L of 10 nmol/L siRNA per mouse). **B**, LLC tumor size at day 7 after injection at multiple intralesional sites. **B1**, control; **B2**, mTERT siRNA:SWNT+ complexes; **B3**, mTERT siRNA alone; **B4**, mock siRNA:SWNT+ complexes. LLC tumor cells ( $1 \times 10^6$  per mouse) were injected s.c into right leg of mouse (five mice per group). After 1 week, when diameter of tumor was  $\sim 5$  mm, mTERT siRNA:SWNTs were injected into tumor at multiple points (100  $\mu$ L of 10 nmol/L siRNA per mouse). At the same time, controls, siRNA alone, or mock siRNA:SWNT+ complexes were also injected into tumor using similar method. **C**, columns, mean tumor weight; bars, SE. Tumor cells from tissues injected by SWNTs-dsDNA-FAM (**D4-D6**) and control SWNTs (**D1-D3**) viewed by fluorescence microscopy (**D2** and **D5**) and flow cytometry analysis (**D3** and **D6**). Black line, tumor cells from uninjected tissue; red line, fluorescence intensity of tumor cells from tissue injected by SWNTs-dsDNA-FAM or control SWNTs. **E**, induction of senescence by mTERT siRNA:SWNT+ after injection into tumor tissue. After mTERT siRNA:SWNTs were injected into tumor at multiple points (100  $\mu$ L of 10 nmol/L siRNA per mouse) for 6 days, senescence-associated  $\beta$ -galactosidase activity tumor sections from different treatment groups were measured as described previously (26).

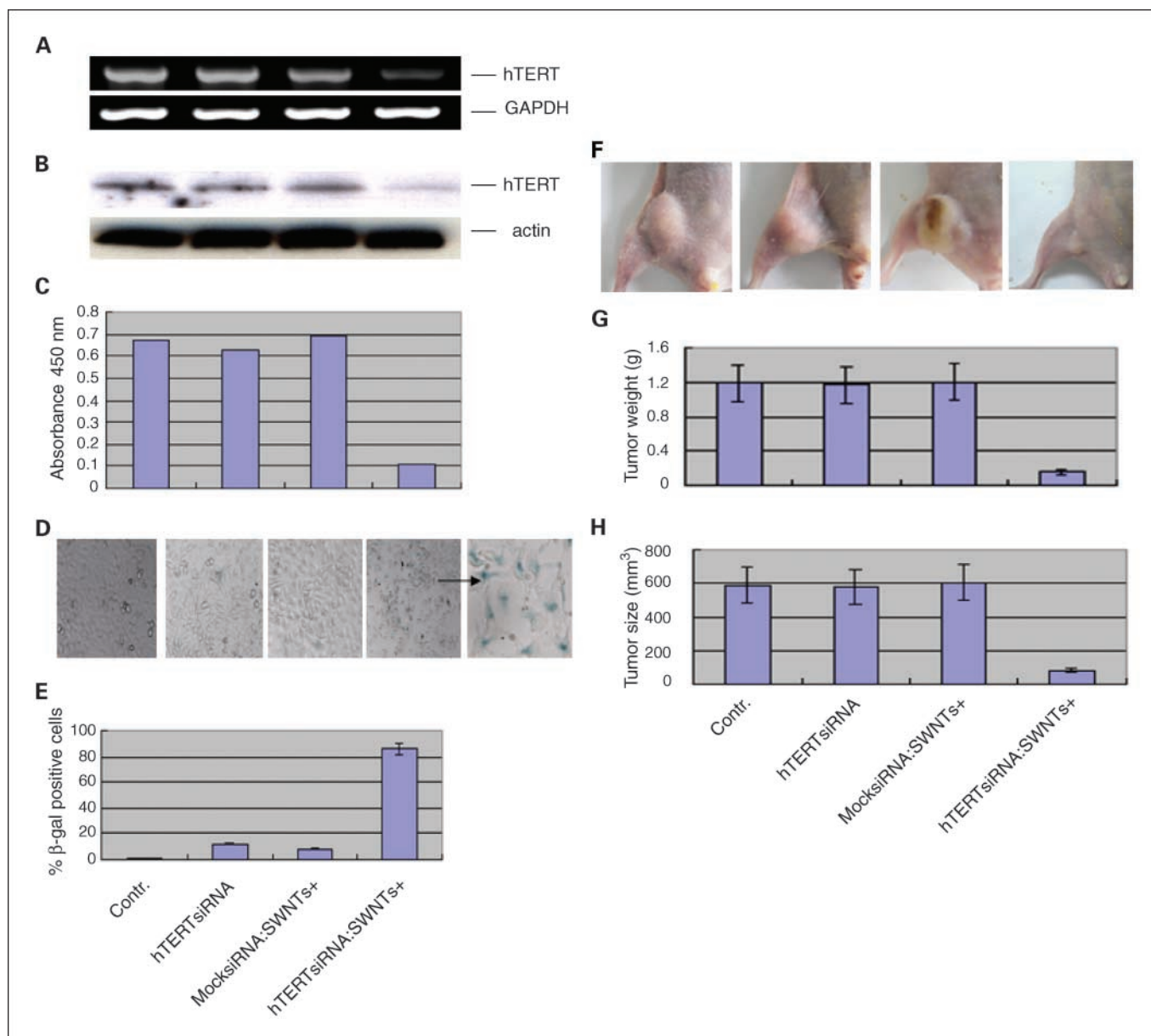


**Fig. 4.** Injection of hTERT siRNA:SWNT+ complexes suppresses HeLa xenograft growth. *A* to *C*, specific gene silencing induced by hTERT siRNA:SWNT+ complexes in human HeLa cells. The level of hTERT transcripts (*A*), hTERT protein (*B*), and telomerase activity (*C*) was assayed in untreated control HeLa cells (*lane 1*) and after treatment of HeLa for 24 hours with 2 nmol/L of mTERT siRNA alone (*lane 2*), mock siRNA:SWNTs+ (*lane 3*), and hTERT siRNA:SWNTs+ (*lane 4*). *D* and *E*, *in vitro* suppression of human HeLa cell proliferation and induction of senescence by hTERT siRNA:SWNT+ complexes; untreated control HeLa cells (*left*) and after treatment of HeLa for 8 days with 2 nmol/L of mTERT siRNA alone (*middle left*), mock siRNA:SWNTs+ (*middle*), and hTERT siRNA:SWNTs+ (*middle right* and *right*). *E*, the number of blue-stained cells was counted in at least 10 fields at  $\times 400$  magnification and expressed as a percentage of total cell number. *F* to *H*, injection of hTERT siRNA:SWNTs+ retarded HeLa tumor growth. HeLa cells ( $2 \times 10^6$  per mouse) were injected s.c into right leg of nude mouse (five mice per group; Beijing Animal Center). After 1 week, when diameter of tumors was  $\sim 2.5$  mm, hTERT siRNA:SWNTs+ or siRNA alone or mock siRNA:SWNT+ complexes were injected into the tumor at multiple points (100  $\mu$ L of 10 nmol/L siRNA per mouse). *F*, one representative of per group of control animals (*left*), hTERT siRNA alone (*middle left*), mock siRNA:SWNT+ (*middle right*), and hTERT siRNA:SWNTs+ (*right*). *G*, columns, mean tumor weight; bars, SE. *H*, columns, mean tumor size; bars, SE.

mechanism responsible for arrest. Li et al. found that cell arrest and apoptosis on ectopic expression of mutant TERT occurs independently of p53 and with limited telomeric shortening. However, TERT knockdown is associated with changes in global gene expression profile indicative of a novel response pathway, including suppression of specific genes implicated in angiogenesis and metastasis (24). A recent study suggests the involvement of the transforming growth factor- $\beta$  signaling pathway in this response (25).

Efficient intracellular transport and delivery of siRNA is critical to the potency and *in vivo* application of RNAi. Our results show that mTERT siRNA:SWNT+ complexes mediated by  $-\text{CONH}-(\text{CH}_2)_6-\text{NH}_3^+\text{Cl}^-$  can penetrate the tumor cells both in culture and in mice to induce the suppression of tumor cells. We provide support for the targeting of TERT in genetic therapy of cancer. However, although we chose to target mTERT in these studies, this approach can clearly be extended to other targets for RNAi. Because the functionalized SWNTs do not

only enter cancer cells, we used direct intratumoral injection. Further studies are needed to assess the distribution of SWNTs after systemic i.v. administration and the potential to target undetected micrometastases. Nevertheless, specific targeting of cancer cells could be achieved in those expressing mutated, fusion, or xenogenic oncogenes, for example, knockdown of human papillomavirus-16 E6 and E7, which triggers apoptosis of cervical cancer cells. This approach might also be applicable in cancer cells that are dependent on dramatically elevated levels of a particular proto-oncogene (e.g., HER-2/*neu* or c-Myc).

In summary, these studies show the potential of functionalization of SWNTs with siRNA mediated by  $-(\text{CONH}-(\text{CH}_2)_6-\text{NH}_3^+\text{Cl}^-)$  for specific gene knockdown *in vivo* and suggest that knockdown of TERT expression using specific siRNA: SWNTs+ complexes warrants further exploration as a potential therapeutic strategy against multiple different tumor types.

## Acknowledgments

We thank Xi Peng for providing the technical support.

## References

- Huang W, Taylor S, Fu K, et al. Attaching proteins to carbon nanotubes via diimide-activated amidation. *Nano Lett* 2002;2:311–4.
- Pantarotto D, Briand JP, Prato M, Bianco A. Translocation of bioactive peptides across cell membranes by carbon nanotubes. *Chem Commun (Camb)* 2004;1:16–7.
- Williams KA, Veenhuizen PT, de la Torre BG, Eritja R, Dekker C. Nanotechnology: carbon nanotubes with DNA recognition. *Nature* 2002;420:761.
- Nguyen C, Delzeit L, Cassell A, Li J, Han J, Meyyappan M. Preparation of nucleic acid functionalized carbon nanotube arrays. *Nano Lett* 2002;2:1079–81.
- Pompeo F, Resasco D. Water solubilization of single-walled carbon nanotubes by functionalization with glucosamine. *Nano Lett* 2002;2:369–73.
- Kam NW, Liu Z, Dai H. Functionalization of carbon nanotubes via cleavable disulfide bonds for efficient intracellular delivery of siRNA and potent gene silencing. *J Am Chem Soc* 2005;127:12492–3.
- Morin GB. The human telomere terminal transferase enzyme is a ribonucleoprotein that synthesizes TTAGGG repeats. *Cell* 1989;59:521–9.
- Sontheimer EJ. Assembly and function of RNA silencing complexes. *Nat Rev Mol Cell Biol* 2005;6:127–38.
- Hazani M, Naaman R, Hennrich F, Kappes M. Confocal fluorescence imaging of DNA-functionalized carbon nanotubes. *Nano Lett* 2003;3:153–5.
- Lv X, Du F, Ma Y, Wu Q, Chen Y. Synthesis of high quality single-walled carbon nanotubes at large scale by electric arc using metal compounds. *Carbon* 2005;43:2020–2.
- Far S, Kossanyi A, Verchere-Beaur C, Gresh N, Taillandier E, Perree-Fauvet M. Bis- and tris-DNA intercalating porphyrins designed to target the major groove: synthesis of acridylbis-arginyl-porphyrins, molecular modelling of their DNA complexes, and experimental tests. *Eur J Org Chem* 2004;8:1781–97.
- Chen J, Hamon MA, Hu H, et al. Solution properties of single-walled carbon nanotubes. *Science* 1998;282:95–8.
- Han G, Tamaki M, Hruby V. Fast, efficient, and selective deprotection of the *tert*-butoxycarbonyl (Boc) group using HCl/dioxane (4 M). *J Pept Res* 2001;58:338–41.
- Roby KF, Taylor CC, Sweetwood JP, et al. Development of a syngeneic mouse model for events related to ovarian cancer. *Carcinogenesis* 2000;21:585–91.
- Dignam JD, Lebovitz RM, Roeder RG. Accurate transcription initiation by RNA polymerase II in a soluble extract from isolated mammalian nuclei. *Nucleic Acids Res* 1983;11:1475–89.
- Kim NW, Piatyszek MA, Prowse KR, et al. Specific association of human telomerase activity with immortal cells and cancer. *Science* 1994;266:2011–5.
- Cherukuri P, Bachilo SM, Litovsky SH, Weisman RB. Near-infrared fluorescence microscopy of single-walled carbon nanotubes in phagocytic cells. *J Am Chem Soc* 2004;126:15638–9.
- Singh R, Pantarotto D, McCarthy D, et al. Binding and condensation of plasmid DNA onto functionalized carbon nanotubes: toward the construction of nanotube-based gene delivery vectors. *J Am Chem Soc* 2005;127:4388–96.
- Fitzgerald MS, Riha K, Gao F, Ren S, McKnight TD, Shippen DE. Disruption of the telomerase catalytic subunit gene from *Arabidopsis* inactivates telomerase and leads to a slow loss of telomeric DNA. *Proc Natl Acad Sci U S A* 1999;96:14813–8.
- Feng J, Funk WD, Wang SS, et al. The RNA component of human telomerase. *Science* 1995;269:1236–41.
- Sachsinger J, Gonzalez-Suarez E, Samper E, Heicappell R, Muller M, Blasco MA. Telomerase inhibition in RenCa, a murine tumor cell line with short telomeres, by overexpression of a dominant negative mTERT mutant, reveals fundamental differences in telomerase regulation between human and murine cells. *Cancer Res* 2001;61:5580–6.
- Li S, Rosenberg JE, Donjacour AA, et al. Rapid inhibition of cancer cell growth induced by lentiviral delivery and expression of mutant-template telomerase RNA and anti-telomerase short-interfering RNA. *Cancer Res* 2004;64:4833–40.
- Kraemer K, Fuessel S, Schmidt U, et al. Antisense-mediated hTERT inhibition specifically reduces the growth of human bladder cancer cells. *Clin Cancer Res* 2003;9:3794–800.
- Li S, Crothers J, Haqq CM, Blackburn EH. Cellular and gene expression responses involved in the rapid growth inhibition of human cancer cells by RNA interference-mediated depletion of telomerase RNA. *J Biol Chem* 2005;280:23709–17.
- Hu B, Tack DC, Liu T, Wu Z, Ullenbruch MR, Phan SH. Role of Smad3 in the regulation of rat telomerase reverse transcriptase by TGF $\beta$ . *Oncogene* 2006;25:1030–41.
- Dimri GP, Lee X, Basile G, et al. A biomarker that identifies senescent human cells in culture and in aging skin *in vivo*. *Proc Natl Acad Sci U S A* 1995;92:9363–7.

# Clinical Cancer Research

## Delivery of Telomerase Reverse Transcriptase Small Interfering RNA in Complex with Positively Charged Single-Walled Carbon Nanotubes Suppresses Tumor Growth

Zhuohan Zhang, Xiaoying Yang, Yuan Zhang, et al.

*Clin Cancer Res* 2006;12:4933-4939.

<b>Updated version</b>	Access the most recent version of this article at: <a href="http://clincancerres.aacrjournals.org/content/12/16/4933">http://clincancerres.aacrjournals.org/content/12/16/4933</a>
<b>Supplementary Material</b>	Access the most recent supplemental material at: <a href="http://clincancerres.aacrjournals.org/content/suppl/2007/01/26/12.16.4933.DC1">http://clincancerres.aacrjournals.org/content/suppl/2007/01/26/12.16.4933.DC1</a>

<b>Cited articles</b>	This article cites 23 articles, 9 of which you can access for free at: <a href="http://clincancerres.aacrjournals.org/content/12/16/4933.full#ref-list-1">http://clincancerres.aacrjournals.org/content/12/16/4933.full#ref-list-1</a>
<b>Citing articles</b>	This article has been cited by 3 HighWire-hosted articles. Access the articles at: <a href="http://clincancerres.aacrjournals.org/content/12/16/4933.full#related-urls">http://clincancerres.aacrjournals.org/content/12/16/4933.full#related-urls</a>

<b>E-mail alerts</b>	<a href="#">Sign up to receive free email-alerts</a> related to this article or journal.
<b>Reprints and Subscriptions</b>	To order reprints of this article or to subscribe to the journal, contact the AACR Publications Department at <a href="mailto:pubs@aacr.org">pubs@aacr.org</a> .
<b>Permissions</b>	To request permission to re-use all or part of this article, use this link <a href="http://clincancerres.aacrjournals.org/content/12/16/4933">http://clincancerres.aacrjournals.org/content/12/16/4933</a> . Click on "Request Permissions" which will take you to the Copyright Clearance Center's (CCC) Rightslink site.